



Simian hemorrhagic fever virus infection of rhesus macaques as a model of viral hemorrhagic fever: Clinical characterization and risk factors for severe disease

Reed F. Johnson^{a,*}, Lori E. Dodd^b, Srikanth Yellayi^c, Wenjuan Gu^d, Jennifer A. Cann^c, Catherine Jett^c, John G. Bernbaum^c, Dan R. Ragland^c, Marisa St. Claire^c, Russell Byrum^c, Jason Paragas^c, Joseph E. Blaney^a, Peter B. Jahrling^{a,c}

^a Emerging Viral Pathogens Section, National Institute of Allergy and Infectious Diseases, National Institutes of Health, Bethesda, MD 20892, USA

^b Biostatistics Research Branch, National Institute of Allergy and Infectious Diseases, National Institutes of Health, Frederick, MD 21702, USA

^c Integrated Research Facility, National Institute of Allergy and Infectious Diseases, National Institutes of Health, Frederick, MD 21702, USA

^d Biostatistics Research Branch, SAIC-Frederick, Inc., National Cancer Institute NCI-Frederick, Frederick, MD 21702, USA

ARTICLE INFO

Article history:

Received 14 July 2011

Returned to author for revision

29 August 2011

Accepted 13 September 2011

Available online 19 October 2011

Keywords:

Hemorrhagic fever virus

Animal model

Pathogenesis

Simian hemorrhagic fever virus

Arterivirus

Coagulopathy

Emerging pathogens

Virus

Hemorrhagic disease

ABSTRACT

Simian Hemorrhagic Fever Virus (SHFV) has caused sporadic outbreaks of hemorrhagic fevers in macaques at primate research facilities. SHFV is a BSL-2 pathogen that has not been linked to human disease; as such, investigation of SHFV pathogenesis in non-human primates (NHPs) could serve as a model for hemorrhagic fever viruses such as Ebola, Marburg, and Lassa viruses. Here we describe the pathogenesis of SHFV in rhesus macaques inoculated with doses ranging from 50 PFU to 500,000 PFU. Disease severity was independent of dose with an overall mortality rate of 64% with signs of hemorrhagic fever and multiple organ system involvement. Analyses comparing survivors and non-survivors were performed to identify factors associated with survival revealing differences in the kinetics of viremia, immunosuppression, and regulation of hemostasis. Notable similarities between the pathogenesis of SHFV in NHPs and hemorrhagic fever viruses in humans suggest that SHFV may serve as a suitable model of BSL-4 pathogens.

Published by Elsevier Inc.

Introduction

The causative agents of viral hemorrhagic fevers (VHF) that affect humans are RNA viruses from the families *Filoviridae*, *Arenaviridae*, *Bunyaviridae*, and *Flaviviridae* including Ebola, Marburg, Lassa, Rift Valley Fever, Crimean–Congo Hemorrhagic Fever, and Omsk Hemorrhagic Fever viruses (Feldmann and Geisbert, 2011; Keshtkar-Jahromi et al., 2011; Paragas and Geisbert, 2006; Peters et al., 1989; Ruzek et al., 2010). Because of the extreme morbidity associated with these emerging viruses and the concern that one or more may be used as bioterrorism agents, efforts to further our understanding of disease pathogenesis and to identify countermeasures have intensified. While numerous studies have defined the clinical, virological, immunological, and pathological manifestations of hemorrhagic fever viruses using non-human primate (NHP) models (Geisbert et al., 2003a; Jaax et al., 1995; Johnson et al.,

1995; Paragas and Geisbert, 2006; Peters et al., 1989), the viral and host molecular mechanisms that control disease severity and outcome remain largely unknown. Furthermore, no licensed therapeutic treatments exist for any VHF. A better understanding of the mechanisms associated with VHF outcome would facilitate the investigation of therapeutic agents. Identification of broad-spectrum treatments targeting common viral or host factors is most desirable because the development of individual therapies for each VHF is hindered by the sporadic nature of the outbreaks and the limited commercial viability of such products.

The necessity for high containment laboratories, for instance, biosafety level- (BSL-) 3 or 4, complicates the investigation of these VHF pathogens. Alternatively, a virus that produces similar disease in NHPs that can be studied under BSL-2 conditions would facilitate studies of VHF viruses by virtue of broader access to the scientific community. SHFV in NHPs might serve as an ideal model for human viral hemorrhagic fevers because SHFV 1) has never been associated with human disease, 2) is a biosafety level BSL-2 pathogen, and 3) has clinical manifestations similar to other hemorrhagic fever viruses.

SHFV is an arterivirus that was first identified in 1964 as the causative agent during an outbreak of hemorrhagic disease in Asian origin

* Corresponding author at: National Institutes of Health, NIAID/EVPS, Bldg 33 Rm 2E19A, 33 North Drive Bethesda MD, USA. Fax: +1 301 480 3322.

E-mail address: johnsonreed@mail.nih.gov (R.F. Johnson).

macaques that occurred at both the National Institutes of Health (NIH, Bethesda, MD) (Allen et al., 1968; Palmer et al., 1968; Tauraso et al., 1968) and the Sukhumi Institute of Experimental Pathology and Therapy in the former USSR (Lapin and Shevtsova, 1971; Shevtsova, 1969b; Shevtsova and Krylova, 1971b). Macaques from both institutes were acquired from the same region of India and housed with African origin primates including patas monkeys, baboons, and African green monkeys (Palmer et al., 1968; Shevtsova, 1969b). During the Sukhumi outbreak, the case fatality rate was 100% over 2 months (Lapin and Shevtsova, 1971; Shevtsova et al., 1975) with disease presenting as a hemorrhagic diathesis and acute diffuse encephalomyelitis (Shevtsova and Krylova, 1971b). During the NIH outbreak, the route of transmission was thought to be iatrogenic: needles that were used for tattooing and tuberculosis testing were shared between the African origin primates and the macaques (Allen et al., 1968; Palmer et al., 1968; Tauraso et al., 1968). Macaques developed high fevers and hemorrhagic diathesis but not acute diffuse encephalomyelitis that was observed at Sukhumi (Allen et al., 1968; Shevtsova and Krylova, 1971a). Mortality occurred in 233 of 1029 macaques in affected rooms over a 2 month period. Initial characterization suggested that all infected NHPs succumbed to disease. However, follow up experiments indicated that macaques can develop asymptomatic infection. Specifically, blood and tissue from an asymptomatic survivor successfully induced a viral hemorrhagic fever in macaques not associated with the initial outbreak (Palmer et al., 1968).

Sporadic SHFV outbreaks of iatrogenic origin have occurred since 1964 with mortality rates reported varying from 11% to as high as 100% (Gravell et al., 1986; London, 1977; Palmer et al., 1968; Tauraso et al., 1970). During SHFV outbreaks in 1972 and 1989 the virus was thought to be spread by both direct and indirect contact between macaques (London, 1977; Renquist, 1990). In the 1989 Ebola-Reston outbreak, SHFV was found in 19 of 49 Ebola-Reston positive macaques that succumbed to hemorrhagic fever (Dalgard et al., 1992).

Analysis of SHFV outbreaks and limited experimental infection of macaques identified common clinical signs including fever, mild facial erythema, and edema as early as 48–72 h post-infection (Abildgaard et al., 1975; Gravell et al., 1986; London, 1977; Palmer et al., 1968). Clinical signs indicative of initial infection developed within 72 h post-inoculation and included depression and petechial rash (Palmer et al., 1968). As the disease progressed, macaques developed facial edema, cyanosis, anorexia, adipia, epistaxis, emesis, dehydration, melena, hematoma, retrobulbar hemorrhage and hematologic signs of coagulopathy (Abildgaard et al., 1975; Allen et al., 1968; Gravell et al., 1986; London, 1977; Palmer et al., 1968; Shevtsova, 1969a; Shevtsova and Krylova, 1971a; Tauraso et al., 1968). Clinically, SHFV-infected macaques developed increased activated partial thromboplastin time (aPTT) and prothrombin time (PT), decreased hematocrit, variations in both complete blood count (CBC) parameters and degrees of thrombocytopenia (Palmer et al., 1968). Most animals succumbed to infection within 10 to 15 days after initial onset of disease.

The primary purpose of this study was to further investigate SHFV as a BSL-2 model of viral hemorrhagic fever, and a secondary goal was to identify factors that were associated with lethal disease. We discovered that disease severity was not associated with dose, with an overall mortality rate of 64%, although statistical power was limited due to group size. Infected NHPs developed disease involving multiple organ systems including the mononuclear phagocyte, circulatory, lymphoid, renal, and hepatic systems. We compared survivors to non-survivors to help identify clinical features of lethal disease and markers that may predict outcome and provide targets for clinical treatment and developing therapeutic options for other VHF. Our comparison of survivors and non-survivors revealed different kinetics of viremia, varying severity and kinetics of immunosuppression, and dysregulation of hemostasis. Backwards matched longitudinal analysis (Dodd et al., in preparation) associated increased AST, ALP, ALT, MCP-1, aPTT and IL-6 concentrations, decreases in ALB, and increased aPTT with lethal disease.

Results

Clinical outcome of SHFV infection

Five groups of rhesus macaques were inoculated intramuscularly with increasing doses of SHFV from 50 to 500,000 PFU and were monitored daily for clinical signs and periodically for physiological, virological, and immunological parameters. The initial goal of these studies was to identify a uniformly lethal dose for SHFV in rhesus macaques. Three independent studies were performed. The first study was a pilot study consisting of 3 NHPs that were given 5000 PFU of SHFV, and the second study was a dose ranging study with 4 groups of 3 NHPs which were given 50, 500, 5000, or 50,000 PFU of SHFV. No dose response was observed in the second study, so a third study was performed with 2 groups of 5 NHPs at 50,000 PFU and 500,000 PFU. Table 1 describes mortality rates and viremia by dose; no differences in mortality by dose or gender were observed, therefore comparisons between survivors and non-survivors were used to evaluate factors that may affect lethal outcome. All NHPs developed clinical signs of severe disease; sixteen of the 25 challenged NHPs progressed to established endpoint criteria (see Materials and methods) and were euthanized.

The most common clinical signs of disease were weight loss (as defined by 10% or greater decrease in body weight from D0), dehydration, edema, lymphadenopathy, petechial rash, and splenomegaly (Table 2). Less common or transient signs were diarrhea, melena, epistaxis, weakness, depression, gingival hemorrhage, and dyspnea. Hematuria was frequently observed at necropsy (15 of 25 animals), and proteinuria was observed in all non-survivors. Hematuria and proteinuria were the only clinical signs associated with mortality ($p=0.0081$, and $p<0.0001$ respectively by Fisher's Exact Test). Common gross necropsy findings included myocardial, pyloric junction, and terminal colon hemorrhage, fibrinous exudates in the lungs and heart, generalized edema, hepatic necrosis, renal necrosis, splenomegaly and bacterial abscesses (Table 3).

SHFV induces a consumption coagulopathy that is consistent with a hemorrhagic disease

Hematology supported a consumption coagulopathy as evidenced by increases in activated partial thromboplastin time (aPTT) and prothrombin time (PT), as well as decreases in hematocrit (HCT), hemoglobin (HGB), and platelet counts (Fig. 1). For non-survivors, mean peak elevations for aPTT and PT, and decreases for HCT, HGB, and platelet counts occurred at days 9 (77.1 s), 9 (18.7 s), 11 (25.2%), 12 (93 g/L), and 9 (119 cells $\times 10^3$ /ml), respectively. For survivors, mean elevation peaks for aPTT, PT, and decreases for HCT, HGB, and platelet counts occurred at days 9 (66.1 s), 9 (18.9 s), 15 (23.8%), 15 (89 g/L), and 17 (134 cells $\times 10^3$ /ml), respectively. The presence of fibrin degradation products (FDP), a characteristic of consumption coagulopathy, was observed in 10/10 NHPs (4 survivors and 6 non-survivors) that comprised the third experiment (data not shown). FDP was detectable in surviving NHPs by day 6 post inoculation and by day 4 post inoculation in non-surviving NHPs. The concentrations of FDP were higher in non-

Table 1
Survival, viremia, and incidence of secondary bacterial infection by dose.

Dose (PFU)	% Moribund (no. moribund/total no.)	Mean day of moribund endpoint (range)	Mean peak viremia (\log_{10} PFU/ml) (range)	Proportion of non-survivors that developed bacteremia ^a
50	66 (2/3)	10.5 (5–16)	5.9 (0.0–6.1)	1/2
500	66 (2/3)	17.0 (15–19)	5.8 (4.7–6.2)	2/2
5000	66 (4/6)	13.5 (9–16)	5.7 (2.8–6.4)	2/4
50,000	75 (6/8)	9.3 (9–16)	5.5 (2.8–6.1)	5/6
500,000	40 (2/5)	12.0 (8–16)	4.7 (2.5–5.0)	2/2

^a Bacteremia was defined as positive by blood culture, presence of abscesses at necropsy, or presence of bacteria in multiple organs during histopathological examination.

Table 2
Summary of clinical findings.^a

Clinical sign	Survivors (incidence (%))	Mean days observed	Non-survivors (incidence (%))	Mean days observed	Significant difference in incidence by Fisher's Exact Test (p-value)
Dehydration	9/9 (100%)	6–16	16/16 (100%)	6.7–11.5	1.0000
Facial and/or scrotal edema	5/9 (56%)	7.5–16.5	11/16 (69%)	9.8–9.6	0.6707
Hematuria ^b	4/9 (44%)		11/11 (100%)		0.0081
Lymphadenopathy	7/8 (88%)	3.8–26	15/16 (94%)	4.3–11.5	1.000
Nares and perineum hemorrhage ^c	2/9 (22%)		3/16 (19%)		1.000
Petechiation of skin	5/9 (56%)	7.6–11.6	10/16 (63%)	9.8–10.8	1.000
Proteinuria ^b	0/9 (0%)		11/11 (100%)		<0.0001
Splenomegaly	3/9 (33%)	15.6–17.3	8/16 (50%)	7.6–13.1	0.6766
Weight Loss ^d	1/9 (11%)	21–36	10/16 (63%)	5–11.4	0.0330

^a Criteria evaluated at each physical exam unless otherwise noted and was included if observed at any physical exam. For a few NHPs, sample collection may have been incomplete and was excluded for analysis as indicated by a lower denominator.

^b Determined at necropsy.

^c Not continually sustained.

^d Weight loss was defined as 10% or greater decrease from Day 0.

survivors than survivors. Backwards matched longitudinal analyses (BMLA) comparing survivors and non-survivors indicated that increased AUC and rate of change of aPTT was associated with lethality (AUC $p=0.0020$, rate of change $p=0.0249$, and peak value $p=0.0744$). Changes in PT, HCT, HGB and platelet concentration did not differ significantly between survivors and non-survivors.

Increased serum concentrations of AST, ALP, and ALT and decreases in ALB were associated with lethal disease

Elevations in the concentrations of AST, ALP, and ALT and decreases in ALB concentrations were observed between survivors and non-survivors (Fig. 2) and statistically associated with lethal disease by backwards matched longitudinal analysis. For non-survivors, mean peak concentrations of AST, ALP, and ALT and peak decrease in ALB occurred at days 10 (1127 g/L), 10 (652 g/L), 9 (156 g/L), and 13 (1.7 g/L), respectively. For survivors, mean peak concentrations of AST, ALP, ALT and peak decrease in ALB occurred at days 8 (408 g/L), 10 (543 g/L), 15 (92 g/L), and 13 (2.3 g/L), respectively. Comparisons of concentrations of AST between survivors and non-survivors using BMLA indicated that increased AUC ($p=0.0014$), rate of change ($p=0.0012$), and peak value ($p=0.0002$), were associated with lethal disease. The AUC analysis of ALP indicated that increased ALP was associated with lethal disease ($p=0.0225$). Additionally, rate of change of ALT ($p=0.0190$) and ALB ($p=0.0073$) were associated with lethal disease.

Table 3
Summary of gross pathological findings.^a

Clinical sign	Survivors (incidence (%))	Non-survivors (incidence (%))	Significant difference in incidence by Fisher's Exact Test (p-value)
Bacterial Abscesses	1/9 (11%)	3/16 (19%)	1.0000
Myocardial hemorrhage	1/9 (11%)	8/16 (50%)	0.0875
Pyloric junction hemorrhage	0/9 (0%)	4/16 (25%)	0.2601
Splenomegaly ^b	2/9 (22%)	7/12 (58%)	0.1842
Terminal colon hemorrhage	1/9 (11%)	9/16 (56%)	0.0405

^a Criteria evaluated at gross necropsy of all subjects. Survivors were necropsied at end of study on day 36.

^b Splenomegaly based upon spleen weight as a twofold change in spleen mass as a percentage of body weight at necropsy using the standard of Davies and Morris (Davies and Morris, 1993).

Immunosuppression is common in SHFV-infected NHPs

Immunosuppression was defined as a 20% or greater decrease in cell count based on CBC/Diff analysis. Results, summarized in Table 4, demonstrate that leukopenia, lymphocytopenia, monocytopenia, and neutropenia were prevalent in both survivors and non-survivors, and there was no indication of statistically relevant differences. However, monocytopenia occurred with twofold greater incidence (88%) in non-survivors when compared to survivors (44%) but was not supported by Fisher's Exact Test ($p=0.0581$). Monocytopenia was also observed earlier in infection with a 7 day duration from median days 2 to 9 for non-survivors. 41.7% of surviving NHPs demonstrated a monocytopenia with a later onset and duration occurring between days 4 and 16. Surprisingly, neutropenia was more common and severe in surviving NHPs, but the difference in incidence and severity was not supported by Fisher's Exact Test ($p=0.2077$). Neutropenia in survivors lasted for 18 days with reductions from 60.1 to 87.1%. Fewer non-surviving NHPs developed neutropenia with a mean duration of 7 days and ranges from 42.3 to 94.0% reduction. Leukopenia and lymphocytopenia demonstrated little difference between survivors and non-survivors.

Plaque reduction neutralizing titer₅₀ (PRNT₅₀) indicates that NHPs developed a variable antibody response

Although, NHPs became immunosuppressed they were able to develop a neutralizing antibody response as shown in Fig. 3. PRNT₅₀ indicated that 13 of 16 non-surviving NHPs developed neutralizing antibody titers of 1:160 or greater by average day 9.5 post-inoculation. Eight of 9 surviving NHPs developed neutralizing antibody titers of 1:160 or greater by average day 9.8. Changes in the peripheral blood mononuclear cell populations and specific T-cell responses were not measured.

MCP-1 and IL-6 are elevated in non-surviving NHPs

Simian hemorrhagic fever virus-infected NHPs typically mounted a pro-inflammatory cytokine response. Of the 24 cytokines and chemokines measured, only IL-1ra, IL-6, IL-8, IL-18, IFN γ , RANTES, MCP-1, and VEGF increased 2-fold above baseline values and were included for analysis. These data are summarized in Table 5. Backwards matched longitudinal analyses were performed on these selected cytokines and indicated that MCP-1 and IL-6 were associated with lethal disease. MCP-1 profiles were elevated for non-survivors over survivors for all 3 comparisons but was suggestive of statistically significant differences for only AUC (AUC $p=0.0285$, rate of change $p=0.1450$, and peak value $p=0.0538$). IL-6

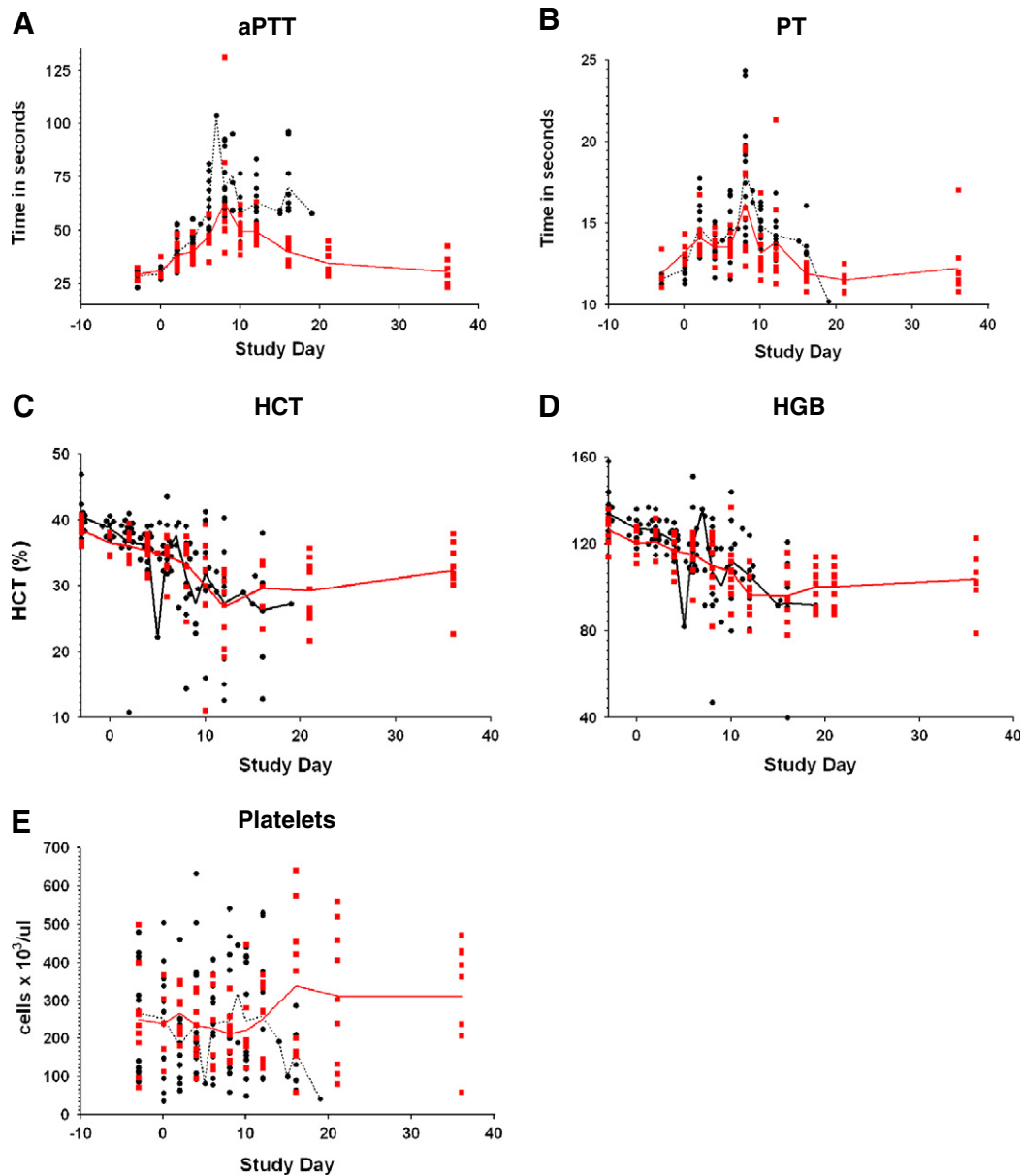


Fig. 1. Hematology supports an SHFV induced consumption coagulopathy. Longitudinal analysis of the daily averages from time of inoculation to study end. The red line represents the daily average of survivors, the black line represents the daily average of non-survivors, data points represent individual NHPs.

profiles were also increased for all 3 comparisons but was suggestive of statistically significant differences for only AUC (AUC $p=0.0485$, rate of change $p=0.0577$, and peak value $p=0.1074$).

Histopathological analysis supports coagulopathy in SHFV infected animals

Major histopathological findings and incidence within groups are shown in Table 6. Histopathological examination of tissues from non-surviving NHPs (16/25) demonstrated myocarditis (Fig. 4A), necrotizing hepatitis (Fig. 4B), interstitial nephritis (Fig. 4C), pulmonary edema and fibrin thrombi (Fig. 4D), thymic necrosis with dystrophic mineralization (Fig. 5A), lymphadenitis (Fig. 5B), and necrotizing splenitis (Fig. 5C). Twelve of 16 non-survivors developed septicemia characterized by suppurative hepatitis, thyroiditis, orchitis (Fig. 4E), encephalitis, pleuropneumonia with intralesional bacteria, and bone

marrow atrophy and necrosis. Septicemia was further confirmed by culturing *Streptococcus. sp* and *Staphylococcus. sp* from the blood of non-survivors (Table 1). Major histopathologic changes in the survivors (9/25) included interstitial pneumonia with fibrosis, lymphoid hyperplasia, interstitial nephritis, non-suppurative meningoencephalitis and myelitis (Fig. 6A). Immunohistochemical analysis of the spleen and brain revealed positive staining for viral antigen in splenic macrophages (Fig. 5D) and neuronal cell bodies, astrocytes, glial cells, and encephalitic lesions (Fig. 6B). The incidence of bacteremia, lymphadenitis, lymphoid depletion and lymphocytolysis of lymph nodes, splenitis with lymphoid depletion, and thymocyte depletion with necrosis and dystrophic mineralization was more common in non-survivors than survivors (Fisher's Exact Test; $p=0.0036$, $p<0.0001$, $p<0.0001$, and $p<0.0001$ respectively). Lymphoid hyperplasia within the spleen and lymph nodes occurred with greater incidence in survivors ($p<0.0001$ and $p<0.0001$) (Table 6).

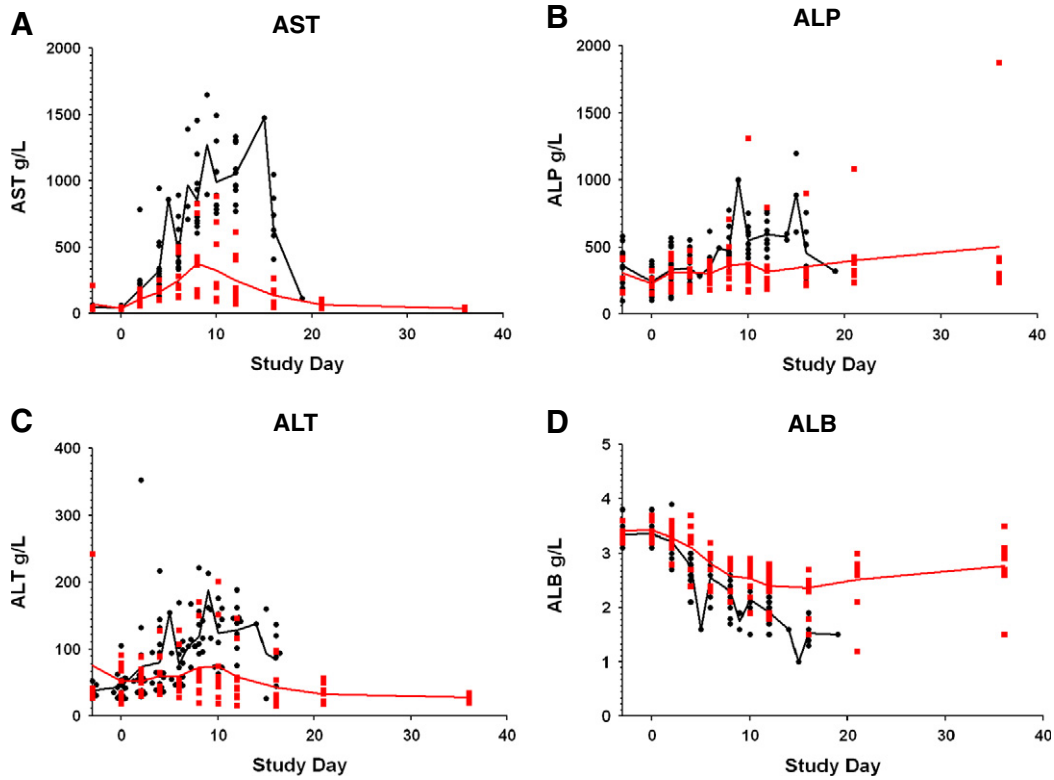


Fig. 2. Serum chemistry values associated with lethality. Longitudinal analysis of the daily averages from time of inoculation to study end. Data points represent individual NHPs, the red line represents the daily average of survivors; the black line represents the daily average of the non-survivors.

Table 4
Immunosuppression in SHFV-infected macaques.

Immunosuppression ^a	Survivors			Non-survivors			Significant difference in incidence by Fisher's Exact Test (p-value)
	Incidence	Mean days of suppression (days post inoculation)	% reduction (range)	Incidence	Mean days of suppression (days post inoculation)	% reduction (range)	
Leukopenia	7/9 (78%)	4–12	60.2 (36.4–79.0)	11/16 (69%)	4–8	47.1 (20–79)	1.0000
Lymphocytopenia	7/9 (78%)	2–10	62.8 (21–79)	12/16 (75%)	2–11	67.1 (50–82)	1.0000
Monocytopenia	4/9 (44%)	4–16	67.7 (31.3–87.5)	14/16 (88%)	2–9	71.6 (47.1–90.3)	0.0581
Neutropenia	7/9 (78%)	4–16	71.9 (60.1–87.1)	7/16 (44%)	4–16	65.5 (42.3–94.0)	0.2077

^a Immunosuppression defined by 20% or greater reduction in cell number post-inoculation.

Transmission electron microscopy suggests endothelial cells and macrophages are targeted by SHFV

Evaluation of the spleen revealed endothelial cell degeneration and necrosis as evidenced by marked cytoplasmic vacuolation, high amplitude mitochondrial swelling, loss of organelles, irregular chromatin clumping and fragmentation, and disintegration of the nuclear and plasma membranes (Fig. 7A). Medium electron dense paracrystalline arrays of viral protein were commonly found within dilated endoplasmic reticulum of degenerate endothelial cells and macrophages (Fig. 7B). Rarely, viral particles were seen within macrophages (Fig. 7C). Viral protein was found within degenerate sinusoidal endothelial cells and macrophages in the liver (data not shown). In many areas throughout the liver, endothelial cells were detached from the basement membrane, cellular debris filled the lumina, and the perivascular adventitia was markedly expanded by abundant electron lucent finely granular acellular material (edema). Lymph node examination further supported viral replication within macrophages as large paracrystalline arrays of viral protein

were commonly found intracytoplasmically (data not shown). Evaluation of the cerebrum also supports endothelial cells as a target cell type because all other cell types present appeared normal with only endothelial cells demonstrating paracrystalline arrays of viral protein (Fig. 7D).

Viral load in tissues supports that SHFV targets the lymphoid, immune, circulatory and hematopoietic systems

Viremia was higher and was present longer in non-surviving NHPs when compared to surviving NHPs (Fig. 8A). Viremia could not be detected past day 10 post-inoculation in surviving NHPs, and survivors had a mean peak viremia of 4.79 log₁₀ PFU/ml that occurred on day 6 post inoculation. Mean peak viremia for non-survivors was 5.66 log₁₀ PFU/ml and occurred on day 7. There was no statistical evidence of an association between increased viremia and disease outcome.

Plaque assays were performed to determine the concentration of infectious virus for 65 tissues. Viral load was observed consistently in 19 tissues from various organ systems. No virus could be detected

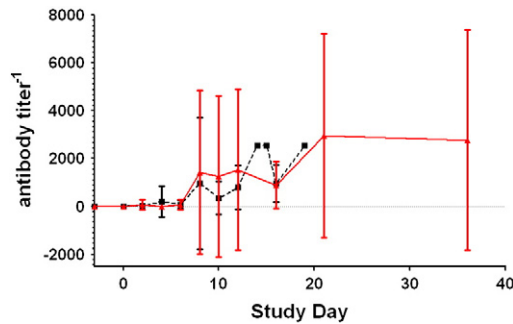


Fig. 3. Plaque reduction neutralizing titer 50%. Longitudinal analysis of the averages of the PRNT₅₀. The red line represents the daily average of survivors; the black line represents the daily average of the non-survivors. The bars indicate the standard deviation.

in surviving NHPs at 36 days post inoculation. The organ systems that developed the highest viral titers were the lymphoid, hematopoietic, circulatory, renal, endocrine, and gastrointestinal systems (Fig. 8B). Analysis of the data suggested a temporal change in virus distribution with NHPs that succumbed prior to and including day 12 post inoculation (7/14 NHPs) demonstrating higher concentrations of live virus in more tissues than NHPs that succumbed past day 12 which only had detectable virus in lung, duodenum, brain and bone marrow; indicating that NHPs were able to reduce viral load in the tissues, but developed other complications induced by SHFV. One such complication is the onset of bacteremia which was statistically associated with lethal disease ($p = 0.0036$) by Fisher's Exact Test. Four of eight NHPs that succumbed prior to and including day 12 post inoculation and 6/6 that succumbed after day 12 were bacteremic based on blood culture at necropsy and histopathological evaluation suggesting a coinfection that may have exacerbated SHFV induced disease.

Discussion

The main purpose of this study was to establish SHFV infection of NHPs as a suitable BSL-2 model of viral hemorrhagic fevers in humans

and define factors associated with disease outcome. Our data support that SHFV LVR induces a viral hemorrhagic fever with similar characteristics as other hemorrhagic fever viruses. Clinical signs of SHFV infection such as edema, petechial rash and coagulopathy were similar to those observed in both human cases and NHP models of EBOV, MARV, CCHFV, and LASV (Carneiro et al., 2007; Cummins, 1991; Feldmann and Geisbert, 2011; Leblebicioglu, 2010). As in filovirus and arenavirus infections, endothelial cells appear to be infected and may play a role in the development of coagulopathy (Hensley and Geisbert, 2005; Kunz, 2009). Monocytes/macrophages also appear to be infected by SHFV, similar to EBOV, MARV, and LASV infections (Lewis et al., 1989; Lukashevich et al., 1999; Stroher et al., 2001). Additionally, the encephalitis and myelitis observed is similar to cases of convalescent human hemorrhagic viral disease (Solbrig and Naviaux, 1997; Walker et al., 1982).

SHFV-induced disease was characterized clinically by petechial rash, edema, perineum hemorrhage, epistaxis, weight loss, and splenomegaly. Hematology indicated evidence of DIC with increases in aPTT, PT, FDP, and decreases in platelet counts, hematocrits, and hemoglobin concentrations. Gross necropsy findings included myocardial, pyloric junction, and terminal colon hemorrhage, splenomegaly, and lymphadenopathy. Histopathologic analysis supported clinical findings with lesions that were indicative of active disease in the heart, kidneys, liver, lung, lymph nodes, spleen, thymus, and CNS. The incidence of lymph nodes with lymphadenitis, lymphoid depletion, and lymphocytolysis, splenitis with lymphoid depletion, and thymocyte depletion with necrosis and mineralization, was significantly increased in non-survivors compared to survivors indicating that disease in these organs is associated with a fatal outcome. Conversely, the incidence of lymphoid hyperplasia occurred with a significantly greater incidence in survivors compared to non-survivors indicates that survivors ultimately developed an effective immune response to viral infection. This finding indicates that intervention aimed at supporting the immune response may help aid survival after infection of VHF. Assessment of viral load further supported the role of the lymphoid and circulatory systems in disease progression. Based on clinical and histopathological disease presentation and organ systems affected we feel that further investigation of SHFV and comparison to other VHF may identify mechanisms of disease shared with other VHF that may lead to broad spectrum therapeutics.

Table 5
Cytokines and chemokines.

Cytokine/chemokine	Group	Mean day of cytokine peak (range)	Mean peak cytokine concentration (pg/ml) (range)	Peak fold change from day zero
IL-1-ra	Survivor	3.78 (2–8)	1309.59 (379.73–4994.85)	329.75
	Non-survivor	8.06 (2–16)	2409.07 (337.98–7386.03)	20419.68
IL-6	Survivor	3.56 (2–16)	97.85 (20.13–434.29)	80.93
	Non-survivor	9.69 (2–19)	1519.51 (72.19–9101.49)	1149.05
IL-8	Survivor	9 (2–21)	708.06 (135.22–1969.26)	9.84
	Non-survivor	4.88 (0–15)	847.25 (185.27–5338.66)	9.84
IL-18	Survivor	3.3 (2–4)	2681.25 (418.17–8541.02)	881.83
	Non-survivor	3 (2–4)	4004.654 (985.98–10742.16)	2303.45
IFN- γ	Survivor	5.56 (2–6)	106.63 (49.39–217.92)	46.28
	Non-survivor	4.06 (2–8)	169.57 (37.32–588.23)	70.81
MCP-1	Survivor	6.4 (2–12)	2797.70 (526.29–4826.65)	31.79
	Non-survivor	5.75 (2–16)	4140.10 (1581.9–5689.92)	40.07
RANTES	Survivor	11.11 (6–21)	150095.5 (25402.41–150095.5)	30.40
	Non-survivor	5.75 (0–10)	66696.84 (6222.8–OOR ^a High)	16.64
VEGF	Survivor	11.56 (4–36)	288.523 (96.72–1355.71)	63.68
	Non-survivor	5.75 (0–15)	170.96 (11.35–500.43)	46.79

^a Out of range.

Table 6
Summary of histopathological findings.^a

Organ	Major finding	Survivor (incidence (%))	Non-survivor (incidence (%))	Significant difference in incidence by Fisher's Exact Test (p-value)
Lung, kidney, liver, heart, GI tract	Bacteremia	1/9 (11%)	12/16 (75%)	0.0036
CNS	Meningitis/encephalitis/myelitis	4/9 (44%)	9/16 (56%)	0.6882
Heart	Myocarditis	9/9 (100%)	15/16 (94%)	1.0000
Kidney	Interstitial nephritis	9/9 (100%)	11/16 (69%)	0.1225
Liver	Necrotizing hepatitis	3/9 (33%)	6/16 (38%)	1.0000
Lung	Interstitial pneumonia fibrin, edema	9/9 (100%)	11/16 (69%)	0.1225
Lymph node	Lymphoid hyperplasia	9/9 (100%)	2/16 (13%)	<0.0001
Lymph node	Lymphadenitis/lymphoid Depletion/lymphocytolysis	0/9 (0%)	12/16 (75%)	<0.0001
Spleen	Lymphoid hyperplasia	7/9 (78%)	1/16 (6%)	<0.0001
Spleen	Splenitis/lymphoid depletion	0/9 (0%)	14/16 (88%)	<0.0001
Thymus	Thymocyte depletion with necrosis and mineralization	0/9 (0%)	14/16 (88%)	<0.0001

^a Criteria evaluated at gross necropsy of all subjects. Survivors were necropsied at end of study on day 36.

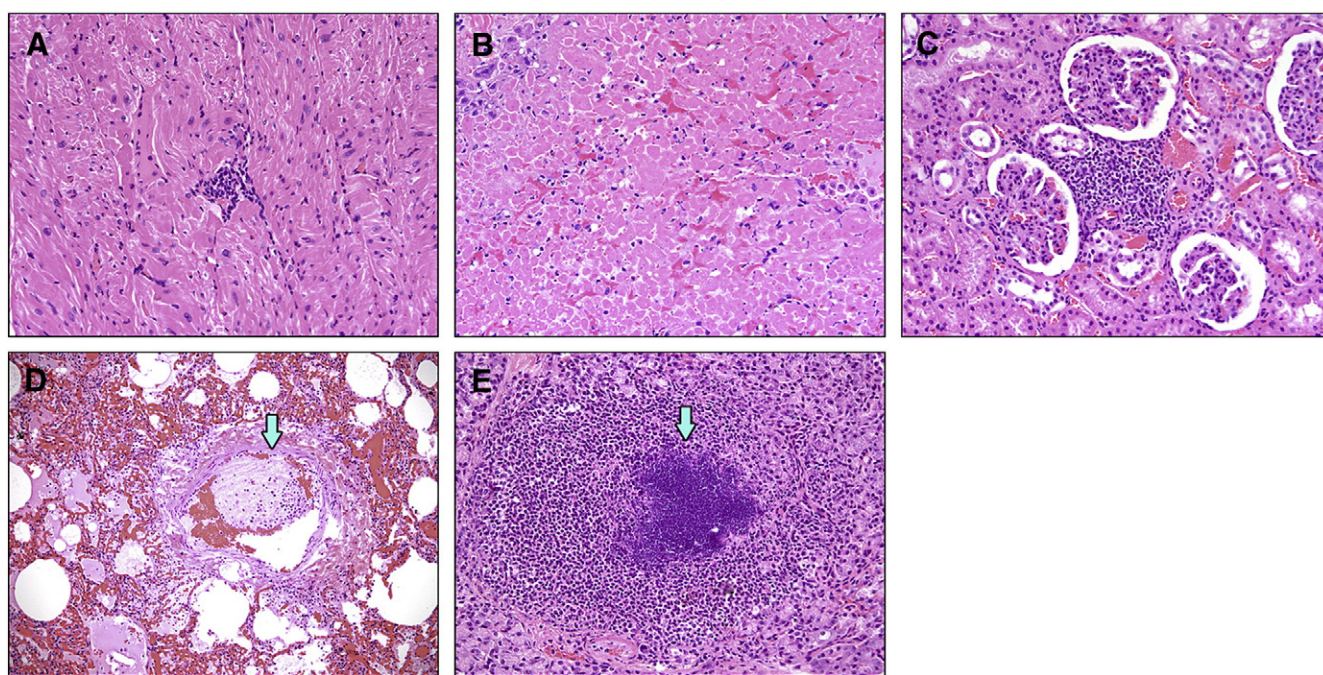


Fig. 4. Select H&E and IHC from non-surviving SHFV infected NHPs. A. Heart: Non-suppurative myocarditis (20×). B. Necrotizing hepatitis. C. Interstitial Nephritis. D. Interstitial pneumonia with thrombus (arrow). E. Abscess of the testis (arrow).

A second goal of this study was to identify host factors statistically associated with lethal disease. Backwards matched longitudinal analyses implicated increases in AST, ALT, ALP, MCP-1, IL-6 and aPTT, and decreases in ALB concentrations associated with progression to lethal disease. Although the serum chemistry analytes were associated with lethal disease, these analyte changes are not specific to one organ or organ system. As such, these data may serve as a predictor for more severe disease and provide a clinical measure that could be easily assessed to evaluate the effectiveness of treatment strategies in real time. Cytokines and other biomarkers such as aPTT that are associated with lethal disease and are also associated with specific host processes (inflammation and clotting) provide targets to further identify host responses leading to severe disease and possibly aid in survival. For example, treatments targeting the coagulation cascade may help improve survival as has been demonstrated for activated protein C treatment of Ebola virus infections of non-human primates (Hensley et al., 2007).

Similar to a recent study of human survivors and non-survivors infected with Ebola virus Zaire, MCP-1 and IL-6 were also associated

with lethal outcome (Wauquier et al., 2010) indicating the utility of the SHFV model for studying the involvement of the cytokine response in VHF pathogenesis. In fact, concentrations and combinations of IL-6, IL-8, IL-18, IFN γ , RANTES, and MCP-1 may support a pro-coagulative state. Although high MCP-1 concentrations have been shown to result in endothelial cell contraction via RhoA signaling (Deshmane et al., 2009), no evidence of endothelial contraction could be found by TEM in our study, perhaps because the samples were collected at necropsy instead of periodically through disease progression. Another possibility is that DIC and infarction are responsible for the observed endothelial cell necrosis. IL-6 has been demonstrated to increase tissue factor expression on monocytes, macrophages, and endothelial cells, (Levi, 2010) thereby initiating coagulation. We hypothesize that in conjunction with endothelial cell disruption, the synergistic effect of IL-6, IL-8, IL-18, IFN γ , RANTES, and MCP-1 could trigger and/or perpetuate the clotting cascade resulting in the observed consumptive coagulopathy. For example, once the clotting cascade is initiated by viral induced endothelial cell death the clotting cascade expands due to increased endothelial cell death as virus

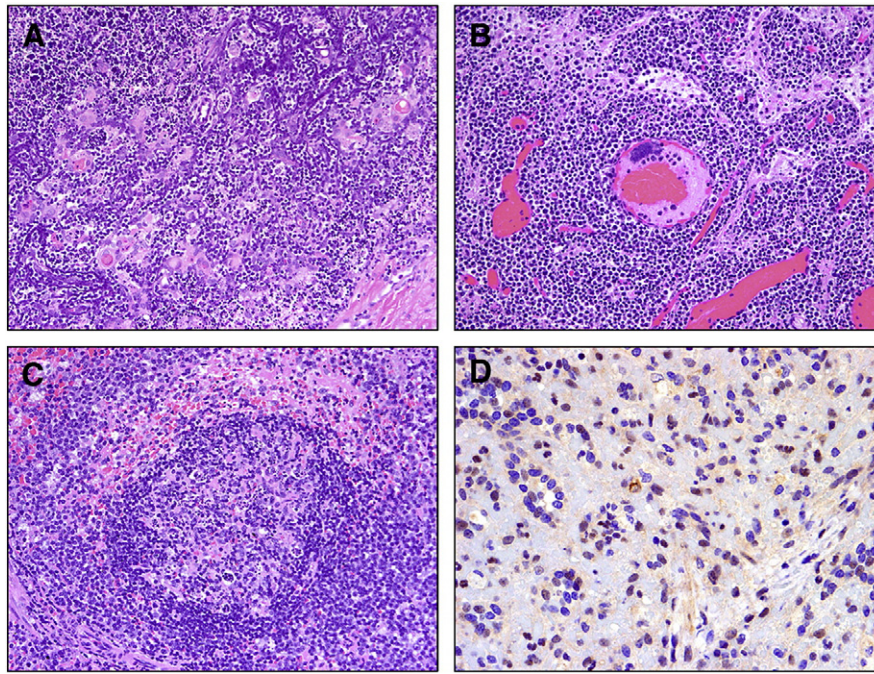


Fig. 5. Select H&E and IHC of lymphoid tissue from non-surviving SHFV infected NHPs. A. Thymocyte depletion with necrosis and mineralization B. Lymphadenitis with lymphoid depletion and lymphocytolysis C. Splenitis with lymphoid depletion D. IHC demonstrating SHFV antigen positive macrophages.

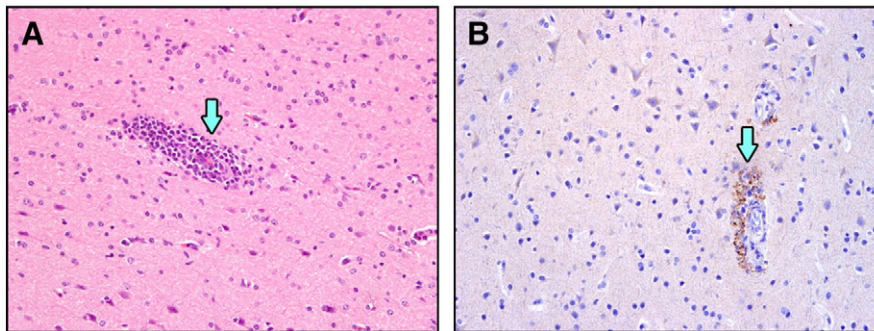


Fig. 6. Select H&E and IHC of cerebrum from SHFV infected NHPs that survived. A. Encephalitis with perivascular cuffing (arrow) B. IHC demonstrating SHFV positive endothelial cells (arrow) with encephalitis.

disseminates causing an increase in the concentrations of the pro-coagulative cytokines. The expansion of the clotting cascade causes thrombin concentrations to increase, resulting in upregulation of MCP-1, IL-6, and other pro-inflammatory cytokines via PARS signaling within endothelial cells and macrophages (Charo and Taubman, 2004; Huerta-Zepeda et al., 2008; van der Poll et al., 2011). The end result is an exacerbation of the coagulopathy. Further experimentation is necessary to delineate the role of MCP-1, IL-6, other cytokines, thrombin, and PARS signaling in the development of hemorrhagic disease.

Previously, Shevtsova et al. were able to demonstrate SHFV antigen in vascular endothelial cells by immunofluorescence (Shevtsova et al., 1975), a finding supported by our data. Infection of endothelial cells and monocytes/macrophages as targets for infection by SHFV was supported by TEM and IHC findings and is similar to that seen in other hemorrhagic fever virus infections (Geisbert et al., 2003b; Kunz, 2009; Lukashevich et al., 1999; Wahl-Jensen et al., 2005). It has been hypothesized that lytic endothelial cell infection contributes to hemorrhagic disease by triggering coagulation via exposure of endothelial collagen as endothelial cells are destroyed (Feldmann and Geisbert, 2011). Our

data suggest that the infection and destruction of endothelial cells initiated a coagulopathy, possibly by exposure of the endothelial collagen and induction of IL-6, MCP-1, and other cytokines. Changes in the vascular permeability would aid the dissemination of SHFV via infected monocytes and macrophages. Immunohistochemistry demonstrated the presence of SHFV antigen, and TEM demonstrated intracytoplasmic paracrystalline arrays of viral protein in endothelial cells. TEM also indicated that hepatic and splenic macrophages were infected by SHFV. SHFV targeting of these cells suggests that infection in both the spleen and liver could result in a release of pro-inflammatory cytokines that would likely alter organ function and vascular permeability.

Another major finding from our study was the high incidence of bacteremia that was significantly associated with lethal disease. Of the 16 NHPs that succumbed to infection, 12 developed secondary bacterial infections and 1/9 non-survivors were found to be bacteremic by the end of the study. The secondary bacterial infection findings in conjunction with the observed immunosuppression and histopathological analysis suggest that study animals developed initial experimental simian hemorrhagic fever followed by onset of bacteremia which exacerbated disease.

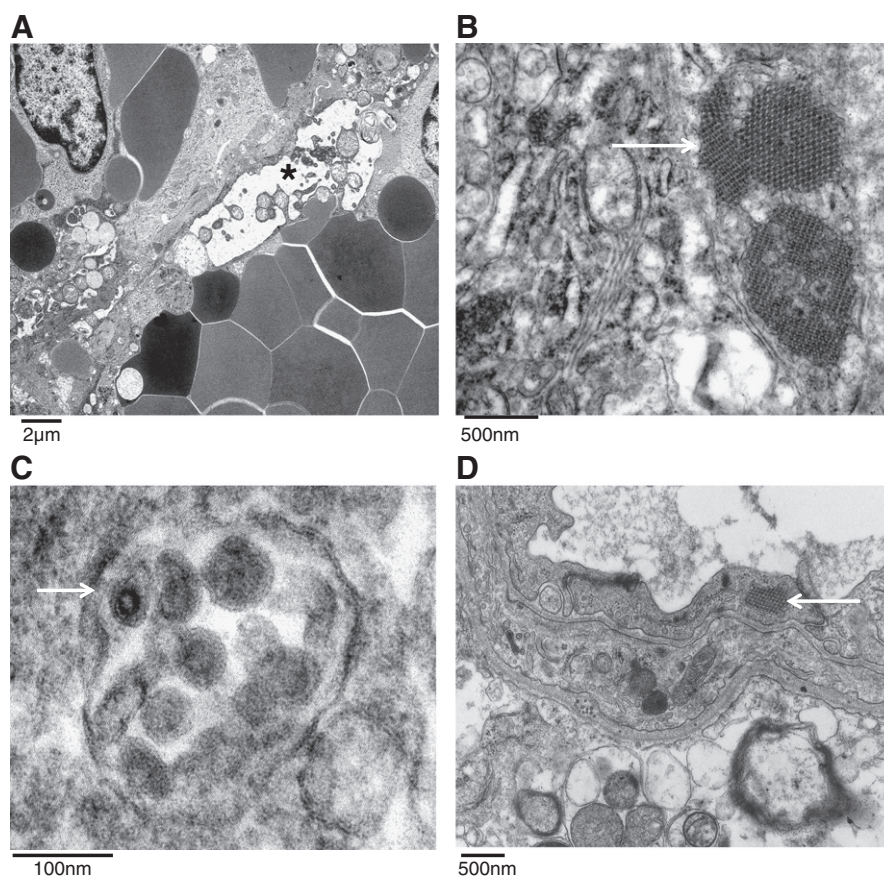


Fig. 7. Transmission electron microscopy of non-surviving SHFV-infected NHPs. A) Sinusoidal endothelial cell degeneration (·) in the spleen. B) Intracytoplasmic paracrystalline arrays of viral protein within a hepatic macrophage. C) Viral particles within the cytoplasm of a splenic macrophage (white arrow). D) Intracytoplasmic paracrystalline arrays of viral protein within an endothelial cell in the brain (white arrow).

Bacterial infections concomitant with SHFV infections have been reported previously (Allen et al., 1968; Renquist, 1990) but systematic study of the role of co-infection during SHFV or any other VHF has not been reported. Given the similar clinical presentation and tissue and cell tropism that SHFV shares with other hemorrhagic fever viruses, it is possible that the immunosuppression of the host during the course of the disease predisposes the subject to opportunistic pathogens. A similar phenomenon could be occurring in human VHFs and case definition possibly under-represents co-infections in the course of disease. Follow up studies in animal models may suffer a similar same fate because the onset of bacteremia may provide grounds for exclusion of study data and the co-infection relegated to an unintended break in procedure. Bacterial infections as a normal, complicating occurrence of human VHF disease is supported by secondary bacterial infections for Junín, Ebola, and hemorrhagic orthopoxvirus infections (Beer et al., 1999; Green et al., 1987; Kempton and Parsons, 1920; Johnson et al., 2011). Further study of SHFV may yield a better understanding of the contribution of secondary bacterial infections to VHF pathogenesis.

SHFV infection results in a disease similar to other viral hemorrhagic fevers. As such, this BSL-2 pathogen provides a model with which to study viral hemorrhagic disease without the constraints of BSL-4 containment and Select Agent restrictions. Key similarities between SHFV and other hemorrhagic fever infections include coagulopathy, upregulation of pro-inflammatory cytokines, involvement of the bone marrow, spleen, lymphoid, and hepatic systems and high mortality rates (64%). Further development of SHFV as a model for hemorrhagic disease may provide insights into the pathogenesis of many other hemorrhagic fever viruses.

Materials and methods

Cells and virus

SHFV strain LVR was initially obtained from ATCC by P.B. Jahrling and passaged 3 times on BSC-1 cells, passaged 1 additional time on MA104 cells followed by propagation in MA104 cells for stock generation: virus was isolated by three rounds of freeze–thaw cycles followed by low speed centrifugation and titration on BSC-1 cells. Virus stocks were tested for sterility by blood agar streak, mycoplasma contamination using Mycosensor (Agilent Technologies Santa Clara CA), endotoxin levels by limulus test (Endosafe-PTS Charles River, Wilmington MA 01887), and cross contamination with other laboratory viruses by PCR (vaccinia and cowpox). Only stocks that were negative by the above testing were used for NHP studies.

Inoculation of NHPs

Twenty-five Rhesus macaques of Chinese and Indian origin were included in the study: 8 females and 17 males with weights ranging from 3.97 kg to 7.91 kg. Prior to study inclusion, NHPs were given a complete physical and screened for antibodies to SHFV, simian retrovirus (SRV), and simian T-lymphotrophic virus (STLV) and only negative NHPs were included. Inocula were diluted in sterile PBS and injected intramuscularly in the quadriceps of the right leg. This study was a compilation of 3 independent experiments. The first study was a pilot with $n=3$ at 5000 PFU of SHFV, the second study included 4 groups of 3 NHPs with doses of SHFV ranging from 50 PFU to 50,000 PFU, the third study included 2 groups of 5 with doses of 50,000 and 500,000 PFU. NHPs were

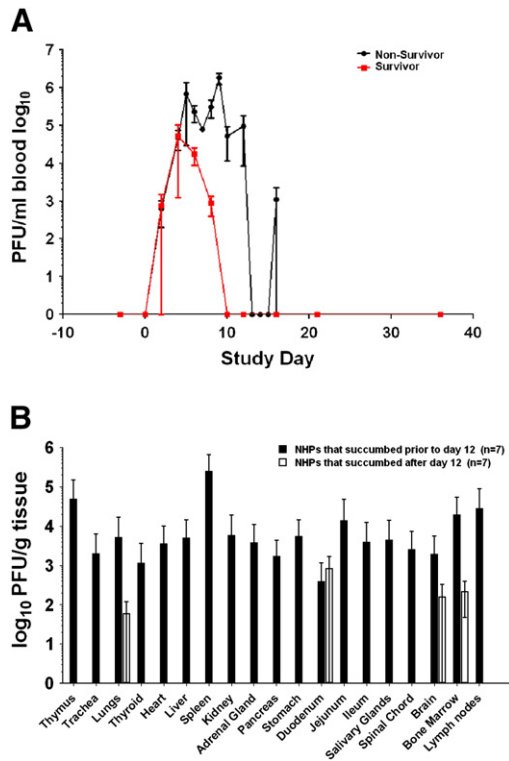


Fig. 8. Viremia and tissue viral load of SHFV infected NHPs. A. Mean virus replication for survivors and non-survivors determined by plaque assay on whole blood (bars represent standard deviation). B. Viral load of non-survivors was measured by plaque assay from indicated tissue homogenates (bars represent standard deviation). Samples for plaque assay were not collected from 2/16 NHPs.

monitored daily for disease progression along with periodic physical exams that included blood draws, nasal and oral swabs, and urinalysis. Moribund clinical endpoint criteria were established as follows: animals were scored on a 0 (normal) to 10-point scale in five broad categories to determine when clinical endpoint criteria had been reached. A score of 10 in any single category, or lower scores which add up to 10 in multiple categories, resulted in immediate euthanasia. The five categories were (1) overall clinical appearance, (2) respiratory abnormalities, (3) activity and behavior, (4) responsiveness, and (5) core body temperatures. All animal experiments were approved by the NIAID Animal Care and Use Committee and adhered to NIH policies.

Plaque assay

The concentration of infectious virus in tissues including whole blood, nasal swabs, and oral swabs was assayed by plaque assay on BSC-1 cell monolayers. Briefly, serial dilutions of 10% or 20% (w/v) tissue homogenates were added onto BSC-1 cell monolayers, overlaid 1 h post-adsorption with 1.8% agarose and 2× MEM (1:1) and incubated at 37 °C, 5% CO₂ for 3 days. Monolayers were fixed with 10% formalin for 1 h followed by removal of the agarose plugs, stained with crystal violet (0.1% crystal violet w/v, 20% methanol v/v), and plaques were enumerated.

Plaque reduction neutralizing titer 50%

The presence of neutralizing antibody was measured by plaque reduction neutralizing titer 50% PRNT₅₀. Serum from the periodic blood draws were diluted 1:10 followed by serial 4 fold dilutions to 1:10,240. 30 PFU of SHFV was incubated with serum and 1× HBSS (CellGro, Manassas, VA) at 37 °C for 1 h. The virus–serum–HBSS mixture was then added to

BSC-1 monolayers overlaid 1 h post-adsorption with 1.8% agarose and 2× MEM (1:1) and incubated at 37 °C, 5% CO₂ for 3 days. Monolayers were fixed with 10% formalin for 1 h followed by removal of the agarose plugs, stained with crystal violet (0.1% crystal violet w/v, 20% methanol v/v), and plaques were enumerated. The serum dilution at which the plaque number was reduced by 50% or greater when compared to controls was scored as the PRNT₅₀ for that sample.

Serology and clinical chemistry

Complete blood counts including leukocyte differentials (CBC/diff) were determined from blood samples collected in ethylenediaminetetraacetic acid (EDTA)-coated blood tubes and analyzed using a Sysmex XS1000i™ (Sysmex America, Mundelein, IL). Serum biochemical analyses were performed using a Piccolo point-of-care blood analyzer with the Comprehensive Metabolic Panel disk (Abaxis, Sunnydale, CA) which included assays for total protein, sodium, potassium, chloride, calcium, glucose, blood urea nitrogen, alkaline phosphatase (ALP), creatine, alanine aminotransferase (ALT), aspartate aminotransferase (AST), albumin (ALB), bilirubin, and carbon dioxide. For coagulation studies, samples were analyzed on a Thromboscreen 2000 (Pacific Hemostasis Fisher Scientific Diagnostics Middletown, VA) for activated partial thromboplastin time (aPTT) and prothrombin time (PT). Fibrin degradation products (FDP) were measured using the Pacific Hemostasis serum FDP kit (Thermo Fisher Scientific, Inc., Middletown, VA) according to manufacturer directions. Serum was collected from SST vacutainers by centrifugation of 1600×g for 10 min. Serum was aliquoted and frozen at –80 °C until study end, and then assayed by latex agglutination. Samples were diluted and mixed in equal volumes with the latex reagent on the test cards provided in the kit. Test cards were gently rocked for 3 min at room temperature, and agglutination results were recorded for each dilution. Results were reported for the highest dilution that yielded a positive agglutination response.

Cytokine and chemokine quantification

The concentrations of 23 cytokines and chemokines in NHP sera were analyzed using the Millipore Non-Human Primate Cytokine Panel Premixed 23-plex (Millipore, Billerica MA). Briefly, undiluted EDTA plasma samples were transferred to a 96-well plate and incubated with beads coated with antibodies directed against each cytokine or chemokine. For the RANTES analysis, a 1:100 dilution was made for each sample. Following incubation, the beads were washed, incubated with anti-cytokine and chemokine antibodies, and incubated with Streptavidin-R-phycoerythrin (SAV/RPE). Beads were assayed on the Bioplex 100 System (Bio-Rad, Hercules CA). Cytokines were included for comparison when there was a two-fold or greater change above background detection of the manufacturer supplied standards.

Necropsy and histology

Complete necropsies were performed either when the NHP met the study endpoint criteria for euthanasia or at study end (day 36). Tissue samples were collected from all major organs for histopathological analysis and determination of viral load. Histology samples were fixed by immersion in 10% phosphate-buffered formalin, paraffin-embedded, and sectioned and affixed to a glass slide. Specimens were then stained with hematoxylin and eosin (H&E), rinsed, and examined via light microscopy by two veterinary pathologists (DRR, SY).

Immunohistochemistry (IHC) was performed on 5 μm thick sections of formalin-fixed paraffin embedded tissue using the Bond automated immunostainer (Leica Microsystems, Bannockburn, IL). Paraffin was removed with xylene, and the sections were rehydrated in a series of alcohol washes. Heat-induced epitope retrieval was performed using citrate (pH 6.0) at 100 °C for 25 min. SHFV antigen was identified immunohistochemically using a biotinylated mouse anti-SHFV polyclonal antibody

(1:100; raised in mice against the nucleocapsid protein sequence CLVNLRYGWQTKNK by Genscript (Piscataway NJ)) incubated for 15 min at room temperature. Primary antibody was localized with horseradish peroxidase and diaminobenzidine substrate. Antibody specificity to SHFV was performed by IHC analysis using the SHFV polyclonal antibody against tissues from historical, normal uninfected NHP controls. In controls to determine background IHC staining, buffer was used in place of the primary antibody. Sections were counterstained with hematoxylin and examined by light microscopy by veterinary pathologists.

Electron microscopy

For thin-section electron microscopic evaluation, dissected tissues were immediately fixed in 2.5% glutaraldehyde and 2.0% paraformaldehyde, in Millonig's sodium phosphate buffer (Tousimis Research, Rockville, MD), for 72 h. Fixed tissue samples were rinsed repeatedly in Millonig's buffer and post-fixed in 1.0% osmium tetroxide in the same buffer. Following rinsing steps in ultrapure water and en bloc staining with 2.0% uranyl acetate, the samples were dehydrated in a series of graded ethanols, infiltrated, and embedded in DER-736 plastic resin (Tousimis Research, Rockville, MD). Embedded blocks were sectioned using a Leica EM UC7 Ultramicrotome. Sections between 50 and 70 nm were collected on 200 mesh copper grids and post-stained with Reynolds's lead citrate. The tissue sections were examined by a veterinary pathologist (JAC) using a FEI Tecnai Spirit Twin transmission electron microscope operating at 80 kV.

Statistical analysis

Survival analyses comparing mortality by inoculation dose and gender were performed using the log-rank test. Hypothesis tests on incidence rates were conducted in Stata 9.0 using Fisher's Exact Test values were considered significant when $p \leq 0.01$.

A total of 60 parameters were assessed during the course of the study. Of these 60, ten parameters were considered subjective (relied on clinical experience i.e. spleen palpation) or did not generate numerical values, two yielded no usable data (nasal and oral swab titers), six were cytokines that did not increase over baseline for any NHP in any dose group, and seven were serum chemistry analytes that did not appreciably change. The remaining 35 parameters (AST, aPTT, ALP, MCP-1, ALT, IL-6, neutrophil counts, platelet count, hematocrits, hemoglobin concentrations, IFN γ , viremia, IL-15, PT, VEGF, IL-5, creatinine, lymphocyte count, sCD40L, GM-CSF, IL-12, total bilirubin, TGf α , IL-2, G-CSF, total protein, IL-8, leukocyte count, monocyte count, IL-18, albumin, MIP-1 α , TNF α , IL-1ra, and RANTES) were considered relevant to disease progression for statistical analysis. Because of the multiple comparisons, the following p-values for test parameters were considered to be supportive of statistical significance for an association with survival status when $p \leq 0.01$, and suggestive of statistical significance when $0.01 \leq p \leq 0.05$. Also, due to the possible correlation between many of the factors, such as cytokines and clotting factors, the p-values was selected *a priori* rather than the Bonferroni method, which is known to be conservative.

To identify factors that may associate with disease severity, changes from baseline were evaluated according to BMLA. The trajectories for a given subject were summarized by the area under the curve (AUC), as this characterizes both the intensity and duration of exposure. Secondary analyses summarized trajectories according to the rate of change (as represented by the slope of a line, over a time period during which change was captured by a line), and the maximum observed value. To compare these summaries between survivors and non-survivors, BMLA compares summary measures over similar time intervals for survivors and non-survivors. Survivors and non-survivors are matched and the summary measures (e.g., AUC) are computed over the same time interval for each pair. The differences in the AUC are computed between the pairs and a paired *t*-test is performed. Because there are many possible pairings, this process is repeated 1000 times, and a common p-value is obtained using the inverse normal p-value averaging (Dodd et al., 2011).

Acknowledgments

This work, in part, was supported by the NIAID and NIAID Division of Intramural Research. We are grateful to Cindy Allan, Krisztina Janosko, Abigail Lara, Erika Zommer, Rebecca Kurnat, Nicholas Oberlander, Isis Alexander, Bernardo Rosa, Oscar Rojas, Haifeng Song, and Kurt Cooper for their contributions to these studies. We thank Sharon Altmann, Stacy Agar, James Lawler, Laura Bollinger, and Fabian De Kok Mercado for their critical review and contribution to the preparation of this manuscript. We would also like to thank Patrick Murray for his assistance with blood culture and bacterial identification.

This project has been funded in whole or in part with federal funds from the National Cancer Institute, National Institutes of Health, under Contract No. HHSN261200800001E. The content of this publication does not necessarily reflect the views or policies of the Department of Health and Human Services, nor does mention of trade names, commercial products, or organizations imply endorsement by the U.S. Government.

References

- Abildgaard, C., Harrison, J., Espana, C., Spangler, W., Gribble, D., 1975. Simian hemorrhagic fever: studies of coagulation and pathology. *Am. J. Trop. Med. Hyg.* 24, 537–544.
- Allen, A.M., Palmer, A.E., Tauraso, N.M., Shelokov, A., 1968. Simian hemorrhagic fever. II. Studies in pathology. *Am. J. Trop. Med. Hyg.* 17, 413–421.
- Beer, B., Kurth, R., Bukreyev, A., 1999. Characteristics of Filoviridae: Marburg and Ebola viruses. *Naturwissenschaften* 86, 8–17.
- Carneiro, S.C., Cestari, T., Allen, S.H., Ramos e-Silva, M., 2007. Viral exanthems in the tropics. *Clin. Dermatol.* 25, 212–220.
- Charo, I.F., Taubman, M.B., 2004. Chemokines in the pathogenesis of vascular disease. *Circ. Res.* 95, 858–866.
- Cummins, D., 1991. Arenaviral haemorrhagic fevers. *Blood Rev.* 5, 129–137.
- Dalgard, D.W., Hardy, R.J., Pearson, S.L., Pucak, G.J., Quander, R.V., Zack, P.M., Peters, C.J., Jahrling, P.B., 1992. Combined simian hemorrhagic fever and Ebola virus infection in cynomolgus monkeys. *Lab. Anim. Sci.* 42, 152–157.
- Davies, B., Morris, T., 1993. Physiological parameters in laboratory animals and humans. *Pharm. Res.* 10, 1093–1095.
- Deshmane, S.L., Kremlev, S., Amini, S., Sawaya, B.E., 2009. Monocyte chemoattractant protein-1 (MCP-1): an overview. *J. Interferon Cytokine Res.* 29, 313–326.
- Dodd, L.E., Johnson, R.F., Blaney, J.E., in preparation. Backward Matched Longitudinal Analysis of Biomarkers Associated with Survival.
- Feldmann, H., Geisbert, T.W., 2011. Ebola haemorrhagic fever. *Lancet* 377, 849–862.
- Geisbert, T.W., Hensley, L.E., Jahrling, P.B., Larsen, T., Geisbert, J.B., Paragas, J., Young, H.A., Fredeking, T.M., Rote, W.E., Vlasuk, G.P., 2003a. Treatment of Ebola virus infection with a recombinant inhibitor of factor VIIa/tissue factor: a study in rhesus monkeys. *Lancet* 362, 1953–1958.
- Geisbert, T.W., Young, H.A., Jahrling, P.B., Davis, K.J., Larsen, T., Kagan, E., Hensley, L.E., 2003b. Pathogenesis of Ebola hemorrhagic fever in primate models: evidence that hemorrhage is not a direct effect of virus-induced cytolysis of endothelial cells. *Am. J. Pathol.* 163, 2371–2382.
- Gravell, M., London, W.T., Leon, M.E., Palmer, A.E., Hamilton, R.S., 1986. Differences among isolates of simian hemorrhagic fever (SHF) virus. *Proceedings of the Society for Experimental Biology and Medicine: Society for Experimental Biology and Medicine*, 181, pp. 112–119.
- Green, D.E., Mahlandt, B.G., McKee Jr., K.T., 1987. Experimental Argentine hemorrhagic fever in rhesus macaques: virus-specific variations in pathology. *J. Med. Virol.* 22, 113–133.
- Hensley, L.E., Geisbert, T.W., 2005. The contribution of the endothelium to the development of coagulation disorders that characterize Ebola hemorrhagic fever in primates. *Thromb. Haemost.* 94, 254–261.
- Hensley, L.E., Stevens, E.L., Yan, S.B., Geisbert, J.B., Macias, W.L., Larsen, T., Daddario-DiCaprio, K.M., Cassell, G.H., Jahrling, P.B., Geisbert, T.W., 2007. Recombinant human activated protein C for the postexposure treatment of Ebola hemorrhagic fever. *J. Infect. Dis.* 196 (Suppl. 2), S390–S399.
- Huerta-Zepeda, A., Cabello-Gutierrez, C., Cime-Castillo, J., Monroy-Martinez, V., Manjarrez-Zavala, M.E., Gutierrez-Rodriguez, M., Izaguirre, R., Ruiz-Ordaz, B.H., 2008. Crosstalk between coagulation and inflammation during Dengue virus infection. *Thromb. Haemost.* 99, 936–943.
- Jaax, N., Jahrling, P., Geisbert, T., Geisbert, J., Steele, K., McKee, K., Nagley, D., Johnson, E., Jaax, G., Peters, C., 1995. Transmission of Ebola virus (Zaire strain) to uninfected control monkeys in a biocontainment laboratory. *Lancet* 346, 1669–1671.
- Johnson, E., Jaax, N., White, J., Jahrling, P., 1995. Lethal experimental infections of rhesus monkeys by aerosolized Ebola virus. *Int. J. Exp. Pathol.* 76, 227–236.
- Johnson, R.F., Yellayi, S., Cann, J.A., Johnson, A., Smith, A.L., Paragas, J., Jahrling, P.B., Blaney, J.E., 2011. Cowpox virus infection of cynomolgus macaques as a model of hemorrhagic smallpox. *Virology* 418 (2), 102–112.
- Kempton, R.M., Parsons, J.P., 1920. Report of a case of hemorrhagic smallpox: a consideration of the role played by the hemolytic Streptococcus. *Arch. Intern. Med.* 26, 594–600.
- Keshkar-Jahromi, M., Kuhn, J.H., Christova, I., Bradfute, S.B., Jahrling, P.B., Bavari, S., 2011. Crimean-Congo hemorrhagic fever: current and future prospects of vaccines and therapies. *Antiviral Res.* 90, 85–92.

- Kunz, S., 2009. The role of the vascular endothelium in arenavirus haemorrhagic fevers. *Thromb. Haemost.* 102, 1024–1029.
- Lapin, B.A., Shevtsova, Z.V., 1971. On the identity of two simian hemorrhagic fever virus strains (Sukhumi and NIH). *Z. Versuchstierkd.* 13, 21–23.
- Leblebicioglu, H., 2010. Crimean–Congo haemorrhagic fever in Eurasia. *Int. J. Antimicrob. Agents* 36 (Suppl. 1), S43–S46.
- Levi, M., 2010. The coagulant response in sepsis and inflammation. *Hamostaseologie* 30 (10–12), 14–16.
- Lewis, R.M., Morrill, J.C., Jahrling, P.B., Cosgriff, T.M., 1989. Replication of hemorrhagic fever viruses in monocytic cells. *Rev. Infect. Dis.* 11 (Suppl. 4), S736–S742.
- London, W.T., 1977. Epizootiology, transmission and approach to prevention of fatal simian haemorrhagic fever in rhesus monkeys. *Nature* 268, 344–345.
- Lukashevich, I.S., Maryankova, R., Vladyko, A.S., Nashkevich, N., Koleda, S., Djavani, M., Horejsh, D., Voitenok, N.N., Salvato, M.S., 1999. Lassa and Mopeia virus replication in human monocytes/macrophages and in endothelial cells: different effects on IL-8 and TNF-alpha gene expression. *J. Med. Virol.* 59, 552–560.
- Palmer, A.E., Allen, A.M., Tauraso, N.M., Shelokov, A., 1968. Simian hemorrhagic fever. I. Clinical and epizootologic aspects of an outbreak among quarantined monkeys. *Am. J. Trop. Med. Hyg.* 17, 404–412.
- Paragas, J., Geisbert, T.W., 2006. Development of treatment strategies to combat Ebola and Marburg viruses. *Expert Rev. Anti Infect. Ther.* 4, 67–76.
- Peters, C.J., Liu, C.T., Anderson Jr., G.W., Morrill, J.C., Jahrling, P.B., 1989. Pathogenesis of viral hemorrhagic fevers: Rift Valley fever and Lassa fever contrasted. *Rev. Infect. Dis.* 11 (Suppl. 4), S743–S749.
- Renquist, D., 1990. Outbreak of simian hemorrhagic fever. *J. Med. Primatol.* 19, 77–79.
- Ruzek, D., Yakimenko, V.V., Karan, L.S., Tkachev, S.E., 2010. Omsk haemorrhagic fever. *Lancet* 376, 2104–2113.
- Shevtsova, Z.V., Karmysheva, V., Chumakov, M.P., 1975. Virological study of simian hemorrhagic fever. *Vopr. Virusol.* 471–476.
- Shevtsova, Z.V., 1969a. Further studies of the virus of simian hemorrhagic fever. *Vopr. Neurokhir.* 33, 604–607.
- Shevtsova, Z.V., 1969b. A further study of simian hemorrhagic fever virus. *Vopr. Virusol.* 14, 604–607.
- Shevtsova, Z.V., Krylova, R.I., 1971a. A comparative study of 2 strains of simian hemorrhagic fever virus. *Vopr. Virusol.* 16, 686–688.
- Shevtsova, Z.V., Krylova, R.I., 1971b. A comparative study of 2 strains of simian hemorrhagic fever virus. *Vopr. Virusol.* 16, 686–688.
- Solbrig, M.V., Naviaux, R.K., 1997. Review of the neurology and biology of Ebola and Marburg virus infections. *Neurol. Infect. Epidemiol.* 2, 5–12.
- Stroher, U., West, E., Bugany, H., Klenk, H.D., Schnittler, H.J., Feldmann, H., 2001. Infection and activation of monocytes by Marburg and Ebola viruses. *J. Virol.* 75, 11025–11033.
- Tauraso, N.M., Shelokov, A., Palmer, A.E., Allen, A.M., 1968. Simian hemorrhagic fever. 3. Isolation and characterization of a viral agent. *Am. J. Trop. Med. Hyg.* 17, 422–431.
- Tauraso, N., Myers, M.G., McCarthy, K., Tribe, G.W., 1970. Simian hemorrhagic fever. In: Balner, H., Beveridge, W.I.B. (Eds.), *Infection and Immunosuppression in Sub-Human Primates*. Munksgaard, Copenhagen, Denmark, pp. 101–109.
- van der Poll, T., de Boer, J.D., Levi, M., 2011. The effect of inflammation on coagulation and vice versa. *Curr. Opin. Infect. Dis.* 24, 273–278.
- Wahl-Jensen, V.M., Afanasieva, T.A., Seebach, J., Stroher, U., Feldmann, H., Schnittler, H.J., 2005. Effects of Ebola virus glycoproteins on endothelial cell activation and barrier function. *J. Virol.* 79, 10442–10450.
- Walker, D.H., Johnson, K.M., Lange, J.V., Gardner, J.J., Kiley, M.P., McCormick, J.B., 1982. Experimental infection of rhesus monkeys with Lassa virus and a closely related arenavirus, Mozambique virus. *J. Infect. Dis.* 146, 360–368.
- Wauquier, N., Becquart, P., Padilla, C., Baize, S., Leroy, E.M., 2010. Human fatal Zaire ebola virus infection is associated with an aberrant innate immunity and with massive lymphocyte apoptosis. *PLoS Negl. Trop. Dis.* 4.